Supporting Information

Carbone *et al.* 10.1073/pnas.0811335106

SI Text

Materials and Characterization. The optimally doped samples of Bi2212 and Bi2223 were grown by the travel solvent floating zone technique, described in ref. 1. The superconducting transition temperature was found to be $T_c = 91$ K in Bi2212 ($\Delta T_c = 1$ K), and $T_c = 111$ K in Bi2223 ($\Delta T_c = 4$ K). The underdoped Bi2212 sample was grown by the self-flux method (2), annealed in an oxygen-deficient atmosphere, and its transition temperature was $T_c = 56$ K ($\Delta T_c < 6$ K). The magnetic susceptibility curves for two representative samples are displayed in Fig. S3.

Intensity Scaling of Bragg Diffractions. In a time-resolved diffraction experiment, different Bragg spots at a given time should exhibit intensity changes in accord with the scattering vectors, s (see Eq. **1**). Therefore, two distinct Bragg diffraction features appearing at $s = s_1$ and s_2 should obey the following scaling relation:

$$\frac{\ln(I_{s_1}/I_0)}{\ln(I_{s_2}/I_0)} = \left(\frac{s_1}{s_2}\right)^2. \qquad [S1]$$

In Fig. S1, we display the intensity changes for two different Bragg spots, recorded in the same pattern, at different scattering vectors. The correct scaling relationship confirms that the observed intensity changes are indeed originated from structural motions.

Three-Temperature Model. Conventionally, the two-temperature model (3) is used to describe laser-induced heating of the electron and phonon subsystems in an elementary metal. Its success is the result of the isotropic electron-phonon coupling in a simple lattice structure, i.e., one atom per primitive unit cell. In complex, strongly correlated materials like high-T_c superconductors, however, such model becomes inappropriate because photoexcited carriers may anisotropically and preferentially couple to certain optical phonon modes, resulting in the failure of assignment of a single temperature to the whole lattice structure.

In the three-temperature model described in ref. 4, in addition to the electron temperature T_e, two temperatures are defined for the lattice part: the hot-phonon temperature, T_p, for the subset of phonon modes to which the laser-excited conduction-band carriers transfer their excess energy, and the lattice temperature, T_l, for the rest of the phonon modes which are thermalized through anharmonic coupling. As an approximation, the spectrum of the hot phonons $F(\Omega)$ is assumed to follow an Einstein model: $F(\Omega) = \delta(\Omega - \Omega_0)$, where δ denotes the Dirac delta function, Ω the energy, and Ω_0 the energy of a hot phonon. Effectiveness of the energy transfer between the carriers and hot phonons is described by the dimensionless parameter λ: $\lambda = 2\int\Omega^{-1}\alpha^2 F d\Omega$, where $\alpha^2 F$ is the Eliashberg coupling function (3). The rate equations describing the temporal evolution of the three temperatures are given by:

$$\frac{dT_e}{dT} = -\frac{3\lambda\Omega_0^3}{\hbar\pi k_B^2}\frac{n_e - n_p}{T_e} + \frac{P}{C_e} \qquad [S2]$$

$$\frac{dT_p}{dt} = \frac{C_e}{C_p}\frac{3\lambda\Omega_0^3}{\hbar\pi k_B^2}\frac{n_e - n_p}{T_e} - \frac{T_p - T_l}{\tau_a} \qquad [S3]$$

$$\frac{dT_l}{dt} = \frac{C_p}{C_l}\frac{T_p - T_l}{\tau_a} \qquad [S4]$$

where $\tau_a = 2.8$ ps is the characteristic time for the anharmonic coupling of the hot phonons to the lattice, n_e and n_p are the electron and hot-phonon distributions given by $n_{e,p} = (e^{\Omega_0/k_B T_{e,p}} - 1)^{-1}$, and P is the laser fluence function; a ratio of 10^3 between the electronic specific heat C_e and the lattice specific heat (C_p and C_l) is known (4).

In our calculations, the values of the parameters were chosen to be the same as in ref. 4, except for the excitation source which in our case has a fluence of 20 mJ/cm^2 and duration of 120 fs. The fit of the simulated lattice temperature to our data gives the following results for the electron-phonon coupling constant in the different samples: $\lambda_{[110]} = 0.12$, $\lambda_{[010]} = 1.0$ and their average $\lambda_{avg} = 0.56$ in underdoped Bi2212; $\lambda_{[110]} = 0.08$, $\lambda_{[010]} = 0.55$ and their average $\lambda_{avg} = 0.31$ in optimally doped Bi2212; $\lambda_{[110]} \approx \lambda_{[010]} = 0.40$ in optimally doped Bi2223. We provide the fits to the data for optimally doped Bi2212 and Bi2223 in Fig. S2.

1. Giannini E, Garnier V, Gladyshevskii R, Flukiger R (2004) Growth and characterization of $Bi_2Sr_2Ca_2Cu_3O_{10}$ and $(Bi,Pb)_2Sr_2Ca_2Cu_3O_{10-\delta}$ single crystals. *Supercond Sci Technol* 17:220–226.
2. Nakamura N, Shimotomai M (1991) Growth of $YBa_2Cu_3O_x$ single crystals by a self-flux method with alkali chlorides as additives. *Physica C* 185:439–440.
3. Allen PB (1987) Theory of thermal relaxation of electrons in metals. *Phys Rev Lett* 59:1460–1463.
4. Perfetti L *et al.* (2007) Ultrafast electron relaxation in superconducting $Bi_2Sr_2CaCu_2O_{8+\delta}$ by time-resolved photoelectron spectroscopy. *Phys Rev Lett* 99:197001.

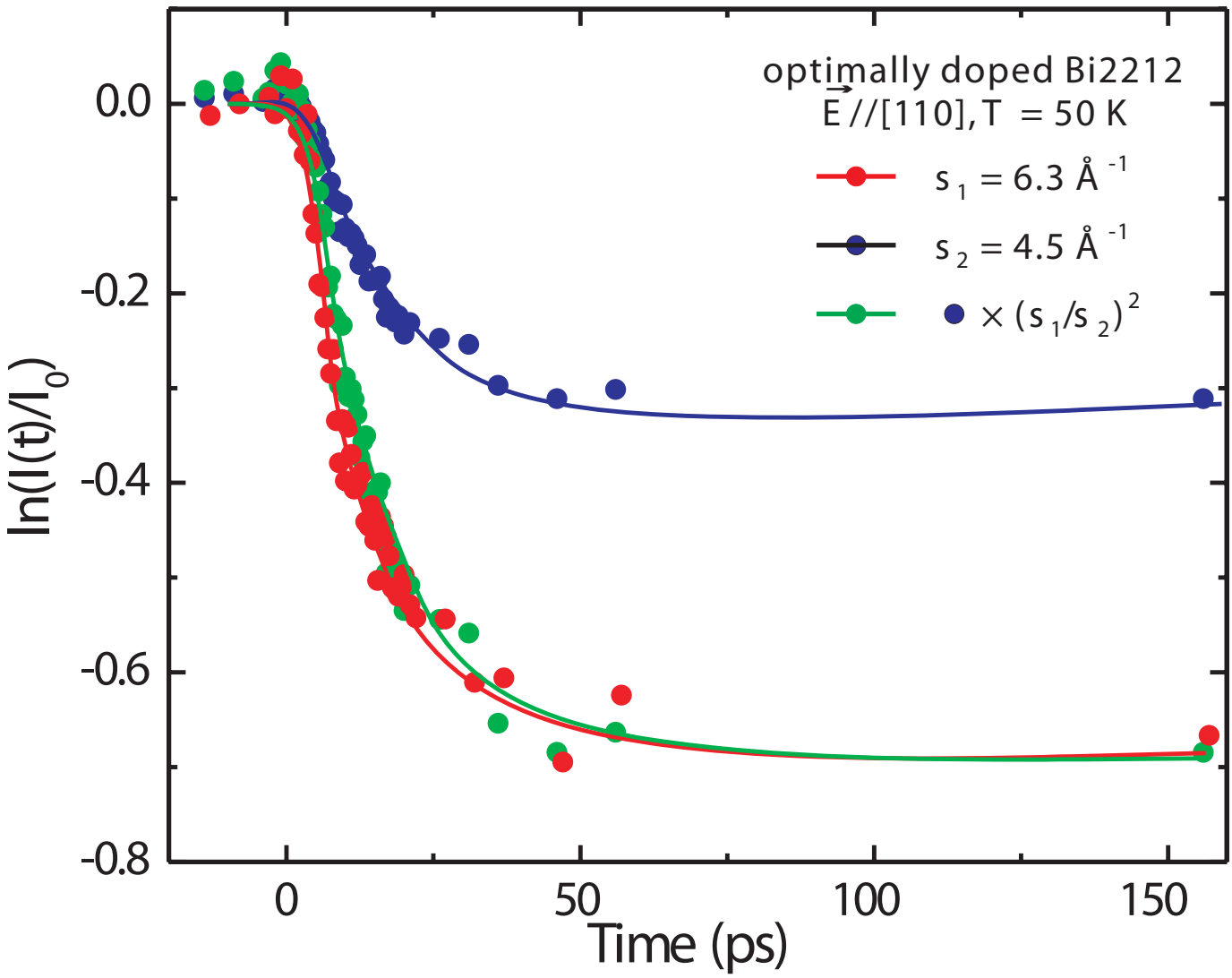

Fig. S1. Intensity scaling between two diffractions. Shown are the decay of two distinct Bragg peaks, observed at $s_1 = 6.3$ Å^{-1} (red) and $s_2 = 4.5$ Å^{-1} (blue). The green curve is obtained by multiplying the data at $s = s_2$ by the factor of $(s_1/s_2)^2$, according to Eq. **S1**, and its match with the data at $s = s_1$ confirms the structurally induced diffraction changes following the carrier excitation.

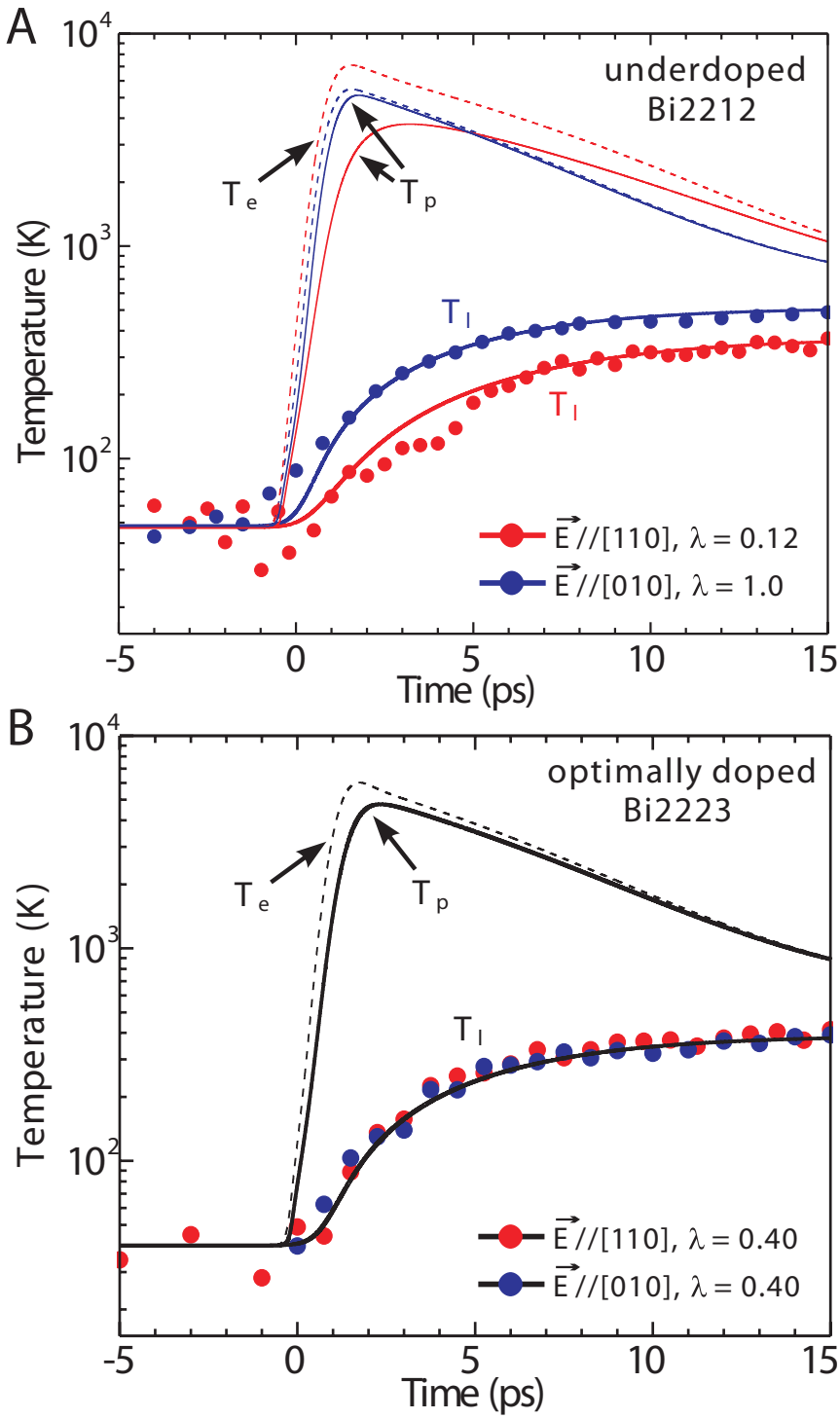

Fig. S2. Lattice temperatures derived from the diffraction intensity data using Eqs. **1** and **2** for different polarizations, along [010] (blue dots) and [110] (red dots), in the underdoped Bi2212 (*A*) and in the optimally doped Bi2223 (*B*). Dashed and solid lines show the calculated temporal evolution of the three temperatures, T_e, T_p and T_l.

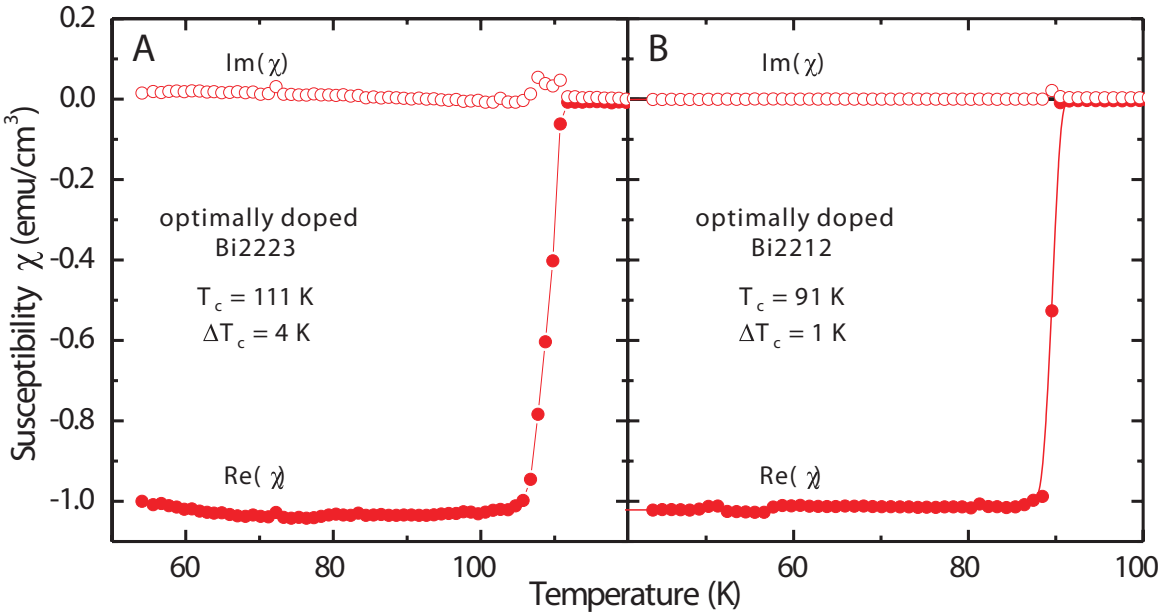

Fig. S3. Sample characterization. (*A*) Temperature dependence of the magnetic susceptibility of an optimally doped Bi2223 sample. (*B*) Temperature dependence of the magnetic susceptibility of a representative optimally doped Bi2212 sample investigated. The sharp transition attests the crystallinity and composition homogeneity of our samples.